ChemPubSoc Europe

DOI: 10.1002/cphc.201402125

Cohesive-Energy-Resolved Bandgap of Nanoscale Graphene Derivatives

Zi Wen,[a] Jinsong Luo,[a, b] Yongfu Zhu,*[a] and Qing Jiang[a]

With a size-dependent cohesive energy formula for two-dimensional coordinated materials, the bandgap variation in quantum dots and nanoribbons of graphene derivatives, such as graphane, fluorographene and graphene oxides, is investigated. The bandgap is found to increase substantially as the diameter or width of the nano-sized material decreases. The bandgap variation is attributed to the change in cohesive energy of edge carbon atoms, and is associated with the physicochemical nature and degree of edge saturation. These predictions agree with previously reported computer simulation results, and have potential application in wide-band optics and optoelectronics.

1. Introduction

Graphene is a 2D sheet composed of carbon atoms arranged in a honeycomb lattice structure, which shows promise as a semiconductor material for future nano- and microelectronics applications,[1,2] such as field-effect transistors (FETs),[3] sensing platforms,[4,5] and optoelectronics.[6] Graphene has zero bandgap, which must be opened for many of these applications. Several methods to open the bandgap have been proposed, such as electrical field manipulation,[7,8] chemical doping,[9,10] or adoption of uniaxial strain.[11,12] However, these methods are limited by their low efficiency and/or incompatibility with common device technologies.[13,14] Alternatively, the bandgap can be opened—by way of the lateral confinement effect—with the formation graphene quantum dots (GQDs) and nanoribbons (GNRs).[1,15–18] With this phenomenon, bandgaps can be in the range 0–1.70 eV for "naked" graphene nanostructures or 0–0.93 eV for those that are H-saturated,[19,20] and therefore meet the requirement of graphene-based FETs. However, such gap sizes cannot be adopted for graphene-based wide-band optics and optoelectronics, as photons of visible light have energies within the 1.6–3.3 eV range. This problem is attributed to the critical size D_c for GQDs or GNRs with $D_c = 1.6$ nm.[21,22] Below this value of D_c, the graphene will suffer from serious edge irregularity and mechanical weakness, which poses a problem for handling and assembly. For their application in optics and optoelectronics, wide band openings can be achieved by forming graphane (GA),[6,23–25] fluorographene (FG)[26,27] or graphene oxide (GO)[28–32] through the reaction of graphene with atomic hydrogen,[33] or with XeF_2 gas[34] or the exfoliation of chemically synthesized graphite oxide.[35] This is possible because, after the functionalization process, sp^2-bonded C atoms are sp^3-bonded, and the electronic properties of GA, FG or GO are therefore changed from those of metals to semiconductors with bandgaps $E_g(\infty)$ larger than 1.7 eV, where ∞ is the bulk size.[36–38]

For their use in nano- and microelectronics, the abovementioned graphene derivatives would be cut into nanoscaled quantum dots (QDs) or nanoribbons (NRs), which are shown in Figure 1A–D (GA and FG) and Figure 1E–H (GO). Because size-dependent properties are a hallmark of nanoscaled materials, it follows that the $E_g(D)$ of those derivative nanostructures can be tuned by changing their size D, which corresponds to the diameter of QDs or the width of NRs. Many contributions in this area have directed efforts to simulations, in which an increase in $E_g(D)$ occurs upon decreasing D.[39] Despite these efforts, however, the nature of the edges of low-dimensional nanostructures of GA, FG and GO and their effects on $E_g(D)$ are still not well understood.[6,23–25] In addition, some fitting exponential expressions, such as $E_g(N) = E_g(\infty) + a/e^{bN}$,[39] elucidated such a dependence on D, where N is defined as the number of C–C dimers for armchair (AC) NRs or the zigzag (ZZ) carbon chains for ZZ-NRs along the NR axis, while a and b are adjustable parameters. However, these fitting expressions cannot be adopted for revealing its essential mechanism on the D-dependences, because a and b vary considerably between different studies. To address this issue, new methods are needed to elucidate $E_g(D)$ in QDs and NRs of graphene derivatives.

Inspired by Lindemann's criterion for the melting of solids and Mott's expression for vibrational melting entropy, Jiang et al. have developed a thermodynamic theory to illustrate the bandgap expansion of 3D coordinated systems.[40,41] Using this model, the bandgap expansion for nanoscaled group III–V and II–VI semiconductors induced by the surface or interface effect has been illustrated successfully.[42–44] Stimulated by this suc-

[a] Prof. Z. Wen, J. Luo, Prof. Y. Zhu, Prof. Q. Jiang
Key Laboratory of Automobile Materials
Ministry of Education, and School of Materials Science and Engineering
Jilin University, Changchun 130022 (China)
Fax: (86) 431-85095371
E-mail: yfzhu@jlu.edu.cn

[b] J. Luo
State Key Laboratory of Luminescence and Applications
Changchun Institute of Optics, Fine Mechanics and Physics
Chinese Academy of Sciences, Changchun 130033 (China)

Supporting Information for this article is available on the WWW under http://dx.doi.org/10.1002/cphc.201402125.

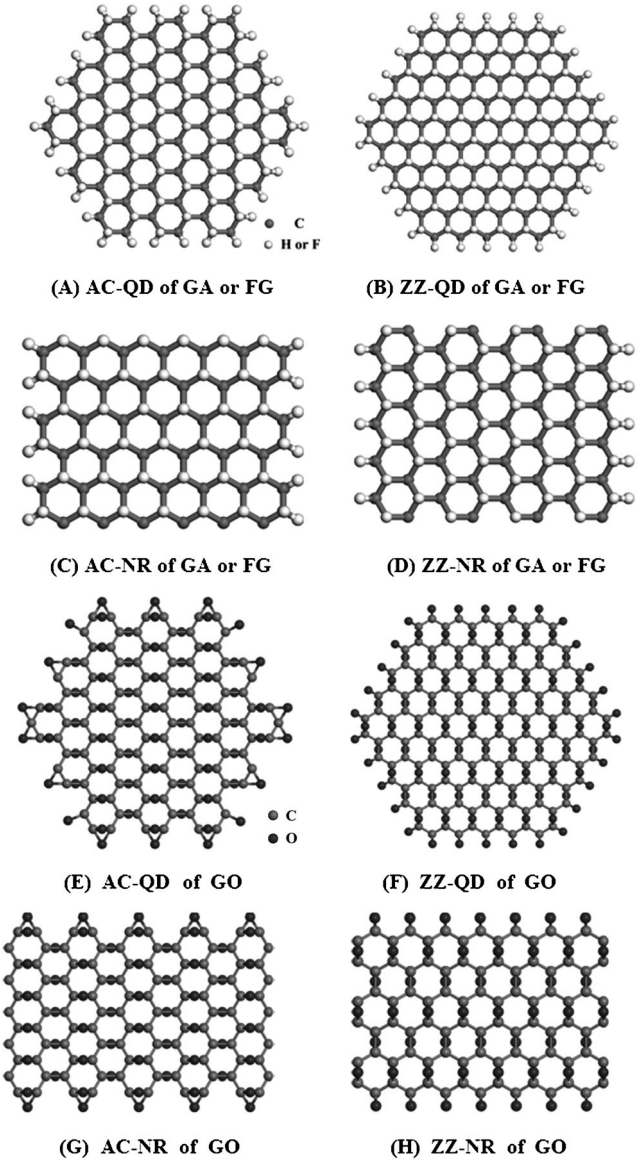

Figure 1. Structures of ideal QDs and NRs of graphene derivatives. A) AC-QDs, B) ZZ-QDs, C) AC-NRs and D) ZZ-NRs for GA or FG. E) AC-QDs, F) ZZ-QDs, G) AC-NRs and H) ZZ-NRs for GO.

cess, we have developed a thermodynamics elucidation of the bandgap openings (BOs) in low-dimensional graphene with the sp^2 configuration of C atoms.[19] The BOs depend on the nature of the edges of graphene nanostructures. When the edges are disordered, $E_g(D)$ is increased monotonically with D. GQDs have larger $E_g(D)$ values than GNRs. In contrast, the value of $E_g(D)$ for nanoporous graphene sheets, which is dependent on D and the geometrical shape of holes, decreases. The BOs can be weakened upon saturation of the edge, relying on the chemical properties of radicals such as H, F or OH. In AC-GNRs with ideal edges, the bandgap opening oscillates. In this work, based on a thermodynamic approach, we have further investigated $E_g(D)$ of QDs and NRs of graphene derivatives with respect to dimension and edge saturation. Significantly, this work provides us new physicochemical insights into the dependence of $E_g(D)$ on D for low-dimensional graphene derivatives.

Calculations

Although the dimensionality of 2D graphene derivatives differs from 3D semiconductors, there exists imperfect coordination of edge C atoms. Accordingly, the coherent energy of edge C atoms will be decreased. The nearly-free-electron approach can also be adopted in predicting the bandgap expansion of graphene derivatives. Therefore, the decrease in atomic cohesive energy, E_c, of edge C atoms will play an essential role in influencing the crystalline field of graphene derivatives, leading to the bandgap expansion. $E_g(D)$ functions of QDs and NRs of GA, FG and GO can therefore be explored with reference to those developed for 3D materials, which can be given as Equation (1):

$$E_g(D) = [2-E_c(D)_{2D}/E_c(\infty)]\,E_g(\infty) \quad (1)$$

According to this equation, $E_g(D)$ of graphene derivatives is related to the change in E_c. Moreover, a function $E_c(D)_{2D}/E_c(\infty)$ for the 2D nanocrystals with free edges having broken bonds is given as Equation (2):

$$E_c(D)_{2D}/E_c(\infty) = \exp[-(\alpha_{2D}-1)/(D/D^0_{2D}-1)] \quad (2)$$

where α_{2D} is a physicochemical quantity that expresses the nature of the edge relative to the interior, and is defined by Equation (3):

$$\alpha_{2D} = \sigma_e(D)^2/\sigma_{in-2D}(D)^2 \quad (3)$$

where σ^2 denotes the mean square displacement of thermal vibration at the melting temperature, and the subscripts e and in-2D refer to the atoms at the edge and the interior, respectively. With regards to D^0_{2D}in Equation (2), it means the critical diameter of a nanocrystal where all the atoms are located at the edge, and is related to the dimensionality or the geometrical shape of the derivative flakes. It can be principally given as Equation (4):

$$D/D^0_{2D} = s/lh, \quad (4)$$

where s/l is the area/edge ratio, which gives $D^0_{2D} = 4h$ for QDs and $D^0_{2D} = 2h$ for NRs with h being the atomic diameter.

When QDs and NRs of graphene derivatives are synthesized, they typically have naked edges. Accordingly, α_{2D} of naked QDs and NRs of graphene derivatives, α^0_{2D}, must be calculated. This calculation is based on that of the 3D with $\alpha^0_{3D} = \sigma_{sv}(D)^2/\sigma_{in-3D}(D)^2$,[40,41] where the subscripts sv and in-3D denote the surface and interior atoms, respectively. Because α^0_{3D} and α^0_{2D} are decided by the coordination imperfection of atoms at the surface of 3D nanocrystals or the edge of 2D graphene flakes, α^0_{2D} can be correlated with α^0_{3D} though the coordination number (CN) of atoms at the surface N_{sv} and that at the edge N_{edge}. According to the inversely proportional relationship between σ^2 and CN of atoms, one has $\alpha^0_{3D} \propto (N_{sv}/N_{in\text{-}3D})^{-1}$ and $\alpha^0_{2D} \propto (N_{edge}/N_{in\text{-}2D})^{-1}$, where $N_{in\text{-}3D}$ and $N_{in\text{-}2D}$ denote the CN in the bulk 3D and 2D crystals, respectively. Thus $\alpha^0_{2D}/\alpha^0_{3D} = (N_{sv}/N_{in-3D})/(N_{edge}/N_{in-2D})$. Because $N_{in-3D} = 12$ and $N_{sv} = 9$ for face-centered cubic and $N_{in-3D} = 8$ and $N_{sv} = 6$ for body-centered cubic crystals,[45] $N_{sv}/N_{in-3D} = 0.75$. Each C atom in GA, FG and GO has an sp^3 configuration, and thus these graphene derivatives have $N_{in-2D} = 4$. When the edges of QDs or NRs are naked, $N_{edge} = 3$, and $N_{edge}/$

$N_{in-2D}=0.75$. Therefore, overall $\alpha^0_{2D}=\alpha^0_{3D}$. Considering the α^0_{3D} expression explored previously,[40,41] one thus has $\alpha^0_{2D}=2S_{vib}(\infty)/3R+1$, where S_{vib} is the vibration entropy. In this expression, $S_{vib}\approx S_m$, where S_m is the melting entropy and R the gas constant. S_m can be obtained with $S_m=H_m(\infty)/T_m(\infty)$ where $H_m(\infty)$ is the melting enthalpy and $T_m(\infty)$ is the melting point. $H_m(\infty)$ and $T_m(\infty)$ are difficult to measure experimentally for GA, FG and GO, therefore their $S_m(\infty)$ values can be referenced to the average of values for graphite and hydrogen, fluorine or oxygen. The structure of GO is complex, therefore, for convenience the fully oxidized GO with a carbon/oxygen ratio of 2:1 is adopted for the calculations here.[46]

In the simulation results as published, the edges of QDs and NRs of the derivatives are saturated with chemical groups R, and α_{2D} is referred to as α^R_{2D}. Upon simulation, α^R_{2D} differs from that of the naked structure, which is denoted by α^0_{2D}. According to the physicochemical nature of the edge, α^R_{2D} can be determined using $\alpha^R_{2D}=\left[E^0_c/E^R_c\right]\alpha^0_{2D}$.[19] To resolve α^R_{2D}, E^0_c and E^R_c should be calculated. For naked QDs or NRs of GA, FG or GO, E^0_c is given as $E^0_c=(N_{edge}/N_{in-2D})^{1/2}E_c(\infty)$,[47] where $N_{edge}/N_{in-2D}=0.75$ as previously stated and $E_c(\infty)=(3E_{C-C}+E_{C-R})/2$ using E_{C-C} and E_{C-R} values from the bulk. If the edges of QDs or NRs are saturated, one edge C atom will have two C–C bonds and two C–R bonds, and $E^R_c(D)$ is given as $E^R_c=E_{C-C}+E_{C-R}$, which is simulated.

2. Results and Discussion

Figure 2 shows the $E_g(D)$ curves as a function of D with naked and saturated AC- or ZZ-QDs (or NRs) of GA, FG and GO. For comparison, the published exponential fitting expressions for assessing the dependence of $E_g(D)$ on D for AC- or ZZ-NRs of GA[39] are also shown in Figure 2D. Available simulation results (symbols, Figure 2B) are shown for verification (also, see Table 1).

Table 1. Parameters necessary to calculate α^0_{2D} and D^0_{2D} for saturated QDs or NRs of GA, FG and GO.[a]

	$H_m(\infty)$ [J mol^{-1}]	$T_m(\infty)$ [K]	S_m [J mol^{-1}K]	h [nm]
GA	-	-	12.287	0.143
FG	–	–	12.361	0.151
GO	–	–	12.271	0.149
H	58.68[48]	14.025[48]	2.09	–
F	255.2[48]	53.48[48]	2.39	–
O	222[48]	54.8[48]	2.03	–

[a] S_{vib} of GA, FG and GO according to $S_{vib}\approx S_m$, where S_m is from C and R with the melting enthalpy $H_m(\infty)$ and the melting point $T_m(\infty)$, using $S_m(\infty)=H_m(\infty)/T_m(\infty)$. As each C atom has three C–C bonds and one C–R bond, $S_m=(3S_{m-C}+S_{m-R})/4$ is used. $S_{m-C}=15.686$ J mol^{-1}K for C is evaluated with values of $H_m(\infty)$ and $T_m(\infty)$ taken from graphite.[49,50] Values of h for GA, FG and GO are adopted from the averaged values for C–C and C–R with $h=(3h_{C-C}+h_{C-R})/4$, where the respective bond lengths are 0.154 and 0.108 nm for C–C and C–H in GA,[23] 0.155 and 0.137 nm for C–C and C–F in FG[51] and 0.151 and 0.144 nm for C–C and C–O in GO.[52]

As Figure 2 shows, $E_g(D)$ is enhanced on the basis of $E_g(\infty)$, as D decreases for naked or saturated QDs and NRs of GA, FG and GO, whereas QDs have larger $E_g(D)$ values than NRs. On decreasing D to $D=D_c=1.6$ nm, $E_g(D)$ is increased from 3.50 eV to 4.97 and 4.17 eV for QD-null and NR-null, respectively, of GA (Figure 2A) and 4.47 and 3.92 eV for QD-H and NR-H, respectively, of GA (Figure 2B); from 3.80 eV to 5.51 and 4.58 eV for QD-null and NR-null, respectively, of FG (Figure 2C) and 4.64 and 4.15 eV for QD-F and NR-F, respectively, of FG (Figure 2D); from 2.40 eV to 3.46 and 2.89 eV for QD-null and NR-null, respectively of GO (Figure 2E) and 3.37 and 2.83 eV for QD-O and NR-O, respectively, of GO (Figure 2F). Note here that null means the edge C atoms are kept naked, and H, F and O

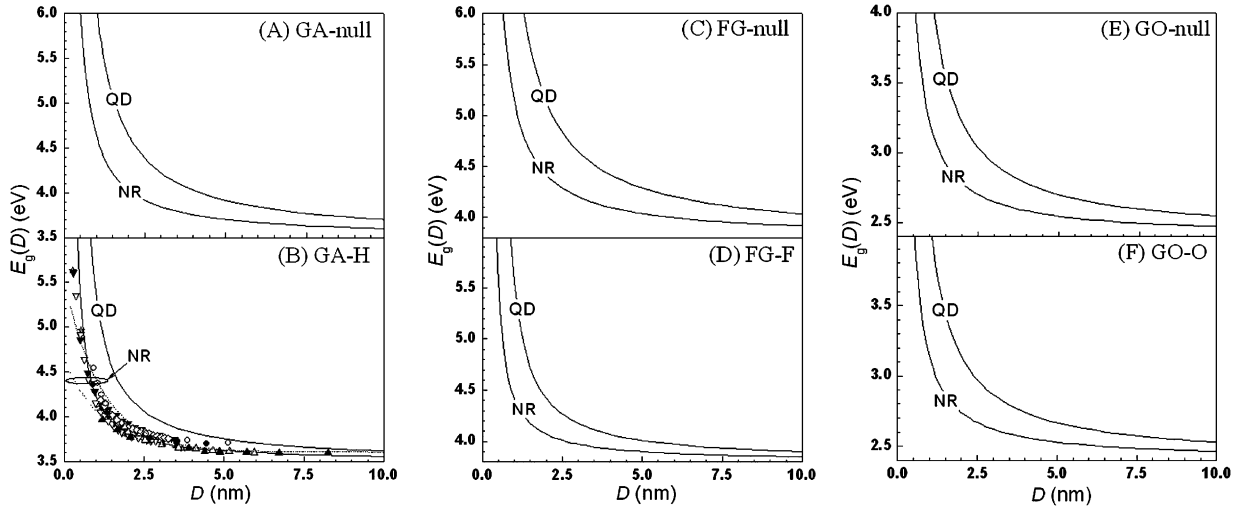

Figure 2. $E_g(D)$ as the function of D in curves derived from Equation (1) for AC- or ZZ-QDs (or NRs) of A) GA-null, B) GA-H, C) FG-null, D) FG-F, E) GO-null and F) GO-O, where $E_c(D)_{2D}/E_c(\infty)$ is calculated using Equation (2). For comparison, the published exponential fitting expressions of $E_g(N)=E_g(\infty)+a/e^{bN}$ to elucidate the dependence of $E_g(D)$ on D with $a=2.15$ eV and $b=0.114$ for AC-NRs and $a=1.18$ eV and $b=0.19$ for ZZ-NRs of GA[39] are also plotted (B) using dashed and/or dotted curves. The symbols in B denote the simulation results of $E_g(D)=E_g(\infty)+\Delta E_g(D)$ with $\Delta E_g(D)$ from the literature: ▲ and △,[39] ▼ and ▽,[25] ◆ and ◇,[6] ● and ○[53] for NRs of GA. The $E_g(\infty)$ values are 3.5, 3.8 and 2.4 eV for GA,[25] FG[54] and GO, respectively.[55,56] Note that, because various $E_g(\infty)$ values (4.38,[53] 3.5[25] and 3.42 eV[6,39]) have been reported for GA with respect to the simulation methods, an average value has been taken. The $E_c(\infty)$ values are 9.49, 7.20 and 8.02 eV for bulk GA, FG and GO, respectively, whereas their corresponding E^R_c values are 10.3, 8.79 and 7.38 eV. The $E_c(\infty)$ and E^R_c values are calculated using the simulation (Supporting Information, and see Table 1 for other necessary parameters).

mean the edge C atoms are saturated by H, F and O atoms, respectively. The increase in $E_g(D)$ is ascribed to the change in the chemical bonding of edge C atoms. These bonds differ from those in the interior, therefore $E_g(D)$ for QDs and NRs of GA, FG or GO is enhanced, as observed. The difference before and after edge saturation suggests that the increase of $E_g(D)$ can be reduced after saturation. The fact that values of $E_g(D)$ for QDs show greater dependence on D than those of NRs is related to the large *l*/*s* ratio of QDs compared to NRs. Our predicted curves correspond well to those derived experimentally, suggesting our predictions are valid. As aforesaid, as shown in Figure 2D, the enhancement of $E_g(D)$ in GA NRs can also be expressed with the reported fits. Due to the presence of adjustable parameters, however, this reported expression cannot be adopted to elucidate the mechanism of the dependence of $E_g(D)$ on D of NRs, nor can it differentiate $E_g(D)$ values of GA and graphene NRs.

In previous studies, we studied the BOs in disordered and ideal GNRs,[19,20] where the impact of edge magnetic interactions was investigated. The magnetic interaction cannot significantly influence the opening in disordered GNRs.[19] In contrast, the inter-edge magnetic interaction has a small influence on the BOs in ZZ-GNRs, although it can make the bandgaps of AC-GNRs oscillate, depending on the width, because of the so-called full-wavelength effect.[20] In comparison, in this work, the inter-edge magnetic interaction should have no contribution to the $E_g(D)$ value of graphene derivative AC- and ZZ-NRs, similar to the disordered case. This is because, in line with published results, ZZ- and AC-NRs of the derivatives with H-saturated edges are nonmagnetic semiconductors. When their edges are naked, AC-NRs are also nonmagnetic, whereas adjacent dangling bonds of ZZ-NRs have antiferromagnetic ordering at that edge.[39] These findings might be related to these derivatives having less π character (i.e. sp^3 configuration of C atoms). Therefore, the monotonic variation of $E_g(D)$ with D for ZZ- and AC-NRs of graphene derivatives (Figure 2) essentially originates from the change in the physicochemical properties at their edges, properties which are associated with the sp^3 configuration of C atoms.

The effect of edge properties—dimension and saturation—on $E_g(D)$ values of GA, FG and GO is essentially decided by the edge coordination imperfection and the change in E_c of edge C atoms. As further evidence for this, Figure 3 shows the plot of $E_g(D)$ as a function of α_{2D} for GA, FG and GO QDs and NRs at $D = 1.6$ nm. It can be seen that $E_g(D)$ increases with α_{2D}. In contrast to NRs, the dependence of $E_g(D)$ on α_{2D} is strong for QDs due to a larger *l*/*s* ratio. When the naked edge of GA, FG and GO QDs and NRs is saturated, $E_g(D)$ is lower. The respective $E_g(D)$ values are 4.97, 5.51 and 3.46 eV for naked QDs of GA, FG and GO. Upon edge saturation, those values decrease to 4.47 eV, 4.64 eV and 3.37 eV, respectively. For GA, FG and GO NR-null, their respective $E_g(D)$ values are 4.17, 4.58, and 2.89 eV. After edge saturation, they decrease to 3.92, 4.15, and 2.83 eV, respectively. These differences indicate further that the expansion of $E_g(D)$ can be weakened after edge saturation.

In view of our theories, the $E_g(D)$ values of the saturated QDs and NRs of graphene derivatives are lowered compared

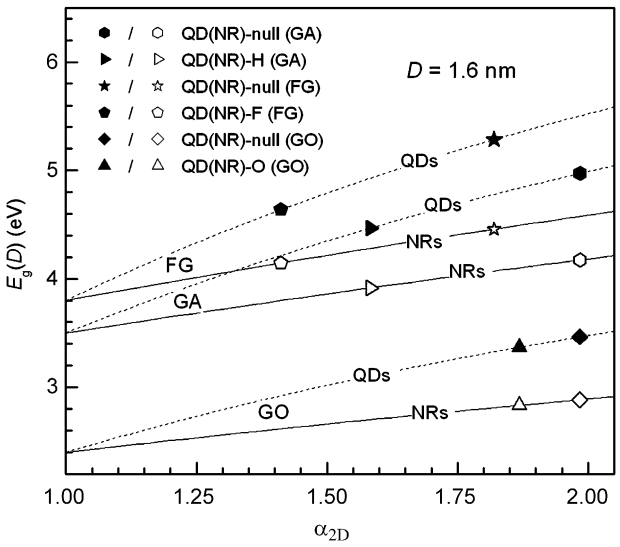

Figure 3. $E_g(D)$ as the function of α_{2D} at $D = 1.6$ nm for AC- or ZZ-QDs (or NRs) of GA, FG and GO using Equations (1) and (2). See Figure 2 for the necessary parameters.

to those of naked QDs. One might thus anticipate that $E_g(D)$ values of QDs and NRs can be adjusted subtly by varying the physicochemical nature of edge C atoms through coverage with R groups; some edge C atoms are saturated, while the others remain naked. Given that there exists a linear relationship between α_{2D} and the degree of edge coverage, the α_{2D} value of QDs and NRs can be given as $\alpha_{2D} = \alpha_{2D}^0(1-x_R) + \alpha_{2D}^R x_R$. In this equation, x_R denotes the fraction of saturated edge C atoms, where $x_R = 0$ indicates the full naked edge state and $x_R = 1$ for a fully edge-saturated structure. Inserting this into Equation (2), $E_g(D)$ of QDs and NRs at different x_R can be plotted for a particular value of D.

Figure 4 shows the $E_g(D)$ curves as functions of x_R upon the edge saturation with H (GA), F (GF) and O (GO, Figure 4A–C respectively). It is predicted that $E_g(D)$ decreases continuously as x_R rises. On increasing x_R from 0 (the full naked edge state) to 1 (the fully edge-saturated state), $E_g(D)$ decreases monotonically as x_R is raised: from 4.97 (QD-null) to 4.47 eV (QD-H), and from 4.17 (NR-null) to 3.92 eV (NR-H) for GA (Figure 4A); from 5.51 (QD-null) to 4.64 eV (QD-F), and from 4.58 (NR-null) to 4.15 eV (NR-F) for FG (Figure 4B); from 3.46 (QD-null) to 3.37 eV (QD-O), and from 2.89 (NR-null) to 2.83 eV (NR-O) for GO (Figure 4C). Strikingly, $E_g(D)$ of nanostructures of graphene derivatives can be modulated subtly by changing their x_R. As well as selecting their size D, this provides a distinct way of tuning $E_g(D)$ values of graphene-based electronic devices.

3. Conclusions

Associated with sp^3 configuration, $E_g(D)$ values of GA, FG and GO QDs and NRs increase on the basis of their $E_g(\infty)$ value as D decreases. The dependence of $E_g(D)$ on D for QDs and NRs varies across different ranges for GA, FG and GO, and is dependent on the degree of edge saturation. The influence of edge geometry on $E_g(D)$ is negligible, whereas the suppression of

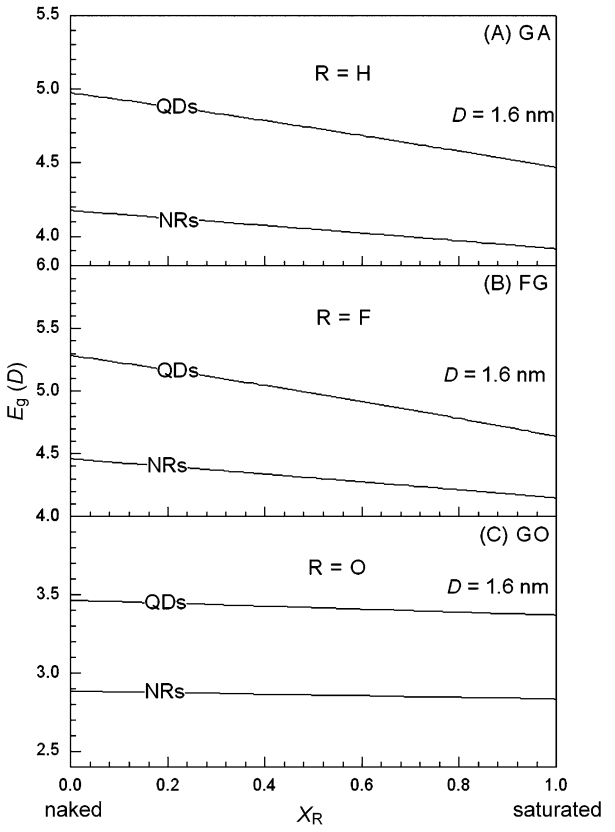

Figure 4. $E_g(D)$ as the function of x_R at $D = 1.6$ nm for QDs and NRs of A) GA, B) FG and C) GO, calculated using Equations (1) and (2). See Figure 2 for the necessary parameters.

$E_g(D)$ expansion from edge saturation should be taken into consideration. The enhancement of $E_g(D)$ is rooted from the change in chemical bonding of C atoms at the graphene or graphene derivative edge.

Acknowledgements

Financial support by the National Key Basic Research Development Program (Grant No. 2010CB631001) is acknowledged.

Keywords: bandgap · cohesive energy · graphene derivatives · quantum dots · thermodynamics

[1] W. T. Zheng, C. Q. Sun, *Energy Environ. Sci.* **2011**, *4*, 627 – 655.
[2] T. Zhang, Q. Z. Xue, S. Zhang, M. D. Dong, *Nano Today* **2012**, *7*, 180 – 200.
[3] T. Ihn, J. Güttinger, F. Molitor, S. Schnez, E. Schurtenberger, A. Jacobsen, S. Hellmüller, T. Frey, S. Dröscher, C. Stampfer, K. Ensslin, *Mater. Today* **2010**, *13*, 44 – 50.
[4] J. Balapanuru, J.-X. Yang, S. Xiao, Q. Bao, M. Jahan, L. Polavarapu, J. Wei, Q.-H. Xu, K. P. Loh, *Angew. Chem. Int. Ed.* **2010**, *49*, 6549 – 6553; *Angew. Chem.* **2010**, *122*, 6699 – 6703.
[5] P. Lazar, S. Zhang, K. Safarova, Q. Li, J. P. Froning, J. Granatier, P. Hobza, R. Zboril, F. Besenbacher, M. D. Dong, M. Otyepka, *ACS Nano* **2013**, *7*, 1646 – 1651.
[6] Y. F. Li, Z. Zhou, P. W. Shen, Z. F. Chen, *J. Phys. Chem. C* **2009**, *113*, 15043 – 15045.
[7] J. B. Oostinga, H. B. Heersche, X. Liu, A. F. Morpurgo, L. M. K. Vandersypen, *Nat. Mater.* **2008**, *7*, 151 – 157.
[8] Y. B. Zhang, T. T. Tang, C. Girit, Z. Hao, M. C. Martin, A. Zettl, M. F. Crommie, Y. R. Shen, F. Wang, *Nature* **2009**, *459*, 820 – 823.
[9] W. J. Yu, L. Liao, S. H. Chae, Y. H. Lee, X. F. Duan, *Nano Lett.* **2011**, *11*, 4759 – 4763.
[10] J. Park, S. B. Jo, Y. J. Yu, Y. Kim, W. Yang, W. H. Lee, H. H. Kim, B. H. Hong, P. Kim, K. Cho, K. S. Kim, *Adv. Mater.* **2012**, *24*, 407.
[11] S. Y. Zhou, G. H. Gweon, A. V. Fedorov, P. N. First, W. A. de Heer, D. H. Lee, F. Guinea, A. H. C. Neto, A. Lanzara, *Nat. Mater.* **2007**, *6*, 770 – 775.
[12] X. H. Peng, S. Velasquez, *Appl. Phys. Lett.* **2011**, *98*, 023112.
[13] M. Burghard, H. Klauk, K. Kern, *Adv. Mater.* **2009**, *21*, 2586 – 2600.
[14] F. Schwierz, *Nat. Nanotechnol.* **2010**, *5*, 487 – 496.
[15] W. Yang, K. R. Ratinac, S. P. Ringer, P. Thordarson, J. J. Gooding, F. Braet, *Angew. Chem. Int. Ed.* **2010**, *49*, 2114 – 2138; *Angew. Chem.* **2010**, *122*, 2160 – 2185.
[16] K. A. Ritter, J. W. Lyding, *Nat. Mater.* **2009**, *8*, 235 – 242.
[17] C. H. Lui, Z. Q. Li, K. F. Mak, E. Cappelluti, T. F. Heinz, *Nat. Phys.* **2011**, *7*, 944 – 947.
[18] M. Y. Han, B. Ozyilmaz, Y. B. Zhang, P. Kim, *Phys. Rev. Lett.* **2007**, *98*, 206805.
[19] Y. F. Zhu, Q. Q. Dai, M. Zhao, Q. Jiang, *Sci. Rep.* **2013**, *3*, 1524.
[20] Y. Zhu, J. Lian, Q. Jiang, *ChemPhysChem* **2014**, *15*, 958 – 965.
[21] K. Bets, B. Yakobson, *Nano Res.* **2009**, *2*, 161 – 166.
[22] V. B. Shenoy, C. D. Reddy, A. Ramasubramaniam, Y. W. Zhang, *Phys. Rev. Lett.* **2008**, *101*, 245501.
[23] J. O. Sofo, A. S. Chaudhari, G. D. Barber, *Phys. Rev. B* **2007**, *75*, 153401.
[24] S. Lebègue, M. Klintenberg, O. Eriksson, M. I. Katsnelson, *Phys. Rev. B* **2009**, *79*, 245117.
[25] D. K. Samarakoon, X. Q. Wang, *ACS Nano* **2009**, *3*, 4017 – 4022.
[26] R. Zboril, F. Karlicky, A. B. Bourlinos, T. A. Steriotis, A. K. Stubos, V. Georgakilas, K. Safarova, D. Jancik, C. Trapalis, M. Otyepka, *Small* **2010**, *6*, 2885 – 2891.
[27] S. H. Cheng, K. Zou, F. Okino, H. R. Gutierrez, A. Gupta, N. Shen, P. C. Eklund, J. O. Sofo, J. Zhu, *Phys. Rev. B* **2010**, *81*, 205435.
[28] D. R. Dreyer, S. Park, C. W. Bielawski, R. S. Ruoff, *Chem. Soc. Rev.* **2010**, *39*, 228 – 240.
[29] K. P. Loh, Q. Bao, G. Eda, M. Chhowalla, *Nat. Chem.* **2010**, *2*, 1015 – 1024.
[30] G. Eda, Y.-Y. Lin, C. Mattevi, H. Yamaguchi, H.-A. Chen, I. S. Chen, C.-W. Chen, M. Chhowalla, *Adv. Mater.* **2010**, *22*, 505 – 509.
[31] J.-A. Yan, L. Xian, M. Y. Chou, *Phys. Rev. Lett.* **2009**, *103*, 086802.
[32] X. Wu, M. Sprinkle, X. Li, F. Ming, C. Berger, W. A. de Heer, *Phys. Rev. Lett.* **2008**, *101*, 026801.
[33] D. C. Elias, R. R. Nair, T. M. G. Mohiuddin, S. V. Morozov, P. Blake, M. P. Halsall, A. C. Ferrari, D. W. Boukhvalov, M. I. Katsnelson, A. K. Geim, K. S. Novoselov, *Science* **2009**, *323*, 610 – 613.
[34] J. T. Robinson, J. S. Burgess, C. E. Junkermeier, S. C. Badescu, T. L. Reinecke, F. K. Perkins, M. K. Zalalutdniov, J. W. Baldwin, J. C. Culbertson, P. E. Sheehan, E. S. Snow, *Nano Lett.* **2010**, *10*, 3001 – 3005.
[35] Y. Zhu, X. Y. Li, Q. J. Cai, Z. Z. Sun, G. Casillas, M. Jose-Yacaman, R. Verduzco, J. M. Tour, *J. Am. Chem. Soc.* **2012**, *134*, 11774 – 11780.
[36] F. Schedin, A. K. Geim, S. V. Morozov, E. W. Hill, P. Blake, M. I. Katsnelson, K. S. Novoselov, *Nat. Mater.* **2007**, *6*, 652 – 655.
[37] X. Wang, L. Zhi, K. Mullen, *Nano Lett.* **2008**, *8*, 323 – 327.
[38] S. Gilje, S. Han, M. Wang, K. L. Wang, R. B. Kaner, *Nano Lett.* **2007**, *7*, 3394 – 3398.
[39] H. Şahin, C. Ataca, S. Ciraci, *Phys. Rev. B* **2010**, *81*, 205417.
[40] Q. Jiang, H. X. Shi, M. Zhao, *J. Chem. Phys.* **1999**, *111*, 2176 – 2180.
[41] Q. Jiang, S. Zhang, M. Zhao, *Mater. Chem. Phys.* **2003**, *82*, 225 – 227.
[42] C. Yang, Q. Jiang, *Mater. Sci. Eng. B* **2006**, *131*, 191 – 194.
[43] Y. F. Zhu, X. Y. Lang, Q. Jiang, *Adv. Funct. Mater.* **2008**, *18*, 1422 – 1429.
[44] S. Li, G. W. Yang, *Appl. Phys. Lett.* **2009**, *95*, 073106.
[45] Q. Jiang, H. M. Lu, *Surf. Sci. Rep.* **2008**, *63*, 427 – 464.
[46] T. Szabó, O. Berkesi, P. Forgó, K. Josepovits, Y. Sanakis, D. Petridis, I. Dékány, *Chem. Mater.* **2006**, *18*, 2740 – 2749.
[47] Y. F. Zhu, W. T. Zheng, Q. Jiang, *Phys. Chem. Chem. Phys.* **2011**, *13*, 21328 – 21332.
[48] http://www.webelements.com.
[49] F. P. Bundy, *J. Chem. Phys.* **1963**, *38*, 618 – 630.
[50] V. N. Korobenko, A. I. Savvatimski, R. Cheret, *Int. J. Thermophys.* **1999**, *20*, 1247 – 1256.

[51] J. C. Charlier, X. Gonze, J. P. Michenaud, *Phys. Rev. B* **1993**, *47*, 16162 – 16168.
[52] J.-A. Yan, M. Y. Chou, *Phys. Rev. B* **2010**, *82*, 125403.
[53] Y. H. Lu, Y. P. Feng, *J. Phys. Chem. C* **2009**, *113*, 20841 – 20844.
[54] K.-J. Jeon, Z. Lee, E. Pollak, L. Moreschini, A. Bostwick, C.-M. Park, R. Mendelsberg, V. Radmilovic, R. Kostecki, T. J. Richardson, E. Rotenberg, *ACS Nano* **2011**, *5*, 1042 – 1046.
[55] H. K. Jeong, M. H. Jin, K. P. So, S. C. Lim, Y. H. Lee, *J. Phys. D* **2009**, *42*, 065418.
[56] G. Eda, M. Chhowalla, *Adv. Mater.* **2010**, *22*, 2392 – 2415.

Received: March 12, 2014
Published online on May 23, 2014